Urania
Jurnal Ilmiah Daur Bahan Bakar Nuklir

Homepage: https://ejournal.brin.go.id/urania

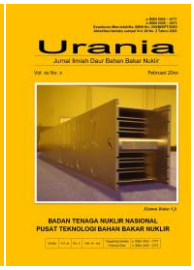

Enhanced U(VI) Adsorption by Ammoniated Sulfonated Covalent Organic Frameworks Synthesized via a Dissolution–Precipitation Method

Rakan Musyafa[1], Edi Nasra[1]*, Aditya Pratama[1], Fiky Putra Dewanda[2], Aubin Athallah Zachran[2], Mahira Salma Azzahra[3], Afiq Azfar Pratama[4], Suci Indryati[4], Ramadhani Amellia[4], Mu'nisatun Sholikhah[5], Deni Mustika[5], Ade Saputra[5]*

[1]Department of Chemistry, Faculty of Mathematics and Natural Sciences, Universitas Negeri Padang, Padang, 25171, Indonesia
[2]Chemical Engineering, Faculty of Industrial Technology, Universitas Pertamina, Jakarta, 12220, Indonesia
[3]Department of Chemistry, Faculty of Science and Technology, UIN Syarif Hidayatullah Jakarta, South Tangerang, 15412, Indonesia
[4]Directorate of Nuclear Facility Management, National Research and Innovation Agency (BRIN), South Tangerang 15314, Indonesia
[5]Research Center for Nuclear Material and Radioactive Waste Technology (PRTBNLR), Research Organization for Nuclear Energy, National Research and Innovation Agency (BRIN), South Tangerang 15314, Indonesia
e-mail: edinasra@fmipa.unp.ac.id; ade.saputra.1@brin.go.id

(Submitted: 25–09–2026, Revised: 19–10–2026, Accepted: 04–11–2026)

ABSTRACT

The development of adsorbent materials with high porosity, large surface area, selectivity, and stability under acidic conditions and elevated temperatures is important for uranium separation. Covalent organic frameworks (COFs), as porous crystalline polymers composed of organic monomers linked by covalent bonds, are promising adsorbents for U(VI). In this study, a sulfonated covalent organic framework (COF-SO_3H) was synthesized by the dissolution–precipitation method using 2,4,6-triformylphloroglucinol and 2,5-diaminobenzenesulfonic acid as precursors, followed by ammoniation using 1% NH_4OH to enhance U(VI) adsorption. The materials were characterized by FTIR, ^{1}H NMR, ^{13}C NMR, PXRD, SEM-EDX, BET, and zeta potential analyses. The synthesis and ammoniation yields were approximately 91% and 75%, respectively. Characterization indicated that ammoniation modified the sulfonate environment and surface charge while preserving the β-ketoenamine framework. Nonlinear regression was used to evaluate adsorption kinetics and isotherms. The pseudo-second-order model provided the better kinetic fit, while the Langmuir model showed the better isotherm fit. The theoretical maximum adsorption capacity increased from 353.42 ± 25.72 to 564.09 ± 44.61 mg/g after ammoniation from initial U(VI) concentrations of 50, 100, 300, 500, 800, and 1000 mg/L, while the Kd value increased from 4.45 × 10^6 to 1.21 × 10^7 mL/g. Temperature-dependent analysis showed that the ammoniated COF achieved its highest adsorption performance at approximately room temperature, whereas the non-ammoniated COF showed increasing adsorption at higher temperatures. Regeneration tests showed only a 9% decrease in adsorption after four cycles. Overall, the results demonstrate that the ammoniation can improve the adsorption performance of the COF toward U(VI).

Keywords: Covalent Organic Framework, ammoniation, dissolution–precipitation, nonlinear regression, uranium adsorption

e-ISSN 2528-0473 | © 2026 The Author(s) | Published by BRIN Publishing
This is an open access article under the CC BY-SA license (https://creativecommons.org/licenses/by-sa/4.0/)

INTRODUCTION

Uranium is an important element that can be used as fuel in nuclear power plants, thereby generating electricity with lower carbon emissions compared to other sources [1]. Uranium is not only sourced from uranium deposits but can also come from other sources. One such source is monazite. Monazite is used to extract rare earth element, but the leaching process produces radioactive waste, including uranium waste. The uranium in monazite itself has a concentration of 15-639.4 ppm. So, it can be said that extracting uranium from monazite sand is still economically viable the minimum uranium concentration in mining deposits is 300 ppm [2].

Adsorption is one approach that can be investigated for recovering dissolved uranium from aqueous solutions. The effectiveness of this process depends on the adsorbent's surface chemistry, accessible adsorption sites, pore structure, and the chemical conditions of the solution. Innovations in adsorbent materials that feature high porosity, large surface area, and stability under acidic conditions and at high temperatures. Examples of such materials include Metal-Organic Frameworks (MOFs) and Covalent Organic Frameworks (COFs). These materials possess a large surface area and functional groups, enabling them to capture U(VI) ions. However, MOFs face stability challenges under acidic conditions [3]. Consequently, COFs show high potential as adsorbents.

Covalent Organic Frameworks (COFs) are a type of porous crystalline polymer material composed of organic monomers linked via covalent bonds. Consequently, COFs possess a large surface area, are porous, and exhibit high chemical and thermal stability. The solvothermal method is commonly used for COF synthesis. This method has several drawbacks, including a lengthy synthesis process and the need for toxic solvents. Consequently, a new method is required. The dissolution-precipitation (DP) method has been developed to reduce reliance on conventional high-temperature solvothermal conditions and enable aqueous, room-temperature synthesis of COFs [4]. Furthermore, subsequent studies demonstrated that the alcohol used during the precipitation process can significantly influence the properties and uranium adsorption performance of DP-derived COFs [5]. These findings indicate that the synthesis route and precipitation medium may affect the resulting material's structure, porosity, and accessibility of functional groups.

The adsorption capacity of COF is influenced by several factors, namely surface area and bound functional groups. COFs containing SO_3H groups have been reported to exhibit superior adsorption capacity compared with COFs bearing other functional groups [6]. It's because sulfonic acid (SO_3H) can undergo deprotonation in aqueous media to form sulfonate groups ($–SO_3^-$). The negatively charged sulfonate groups and their oxygen atoms may interact with U(VI) species through electrostatic association and potentially coordination-related interactions, depending on the pH and uranium speciation. The adsorption capacity of SO_3H-functionalized COF was found to increase after ammonia modification. This improvement is attributed to the introduction of NH_4^+ counterions associated with negatively charged sulfonate groups, which modify the local ionic environment of the adsorbent and promote enhanced adsorption performance [3]. Such modification may influence the surface electrochemical properties and interactions between the adsorbent and U(VI). However, that study employed the solvothermal method, which is inefficient and requires the use of toxic solvents.

This has led to a research gap regarding the effect of ammoniation modification on COF SO_3H synthesized via the DP method using isopropanol as the precipitation medium. Therefore, the present study investigates whether ammoniation changes the U(VI) adsorption performance of a sulfonated COF synthesized using the DP method with isopropanol as the precipitation medium. The novelty of this work lies in evaluating ammoniation-induced changes in the adsorption behaviour and physicochemical properties of this COF.

METHODOLOGY

Material And Equipment

Several materials were used for the synthesis, modification, and adsorption experiments, such as 2,4,6-

 DOI: https://doi.org/10.55981/urania.2026.17361

triformylphloroglucinol (>98.0%, TCI), 2,5-diaminobenzenesulfonic acid, imidazole (>97.0%, Sigma-Aldrich), deionized water, isopropanol (≥99.5%), N, N-dimethylformamide (DMF, ≥99.8%), and methanol. To modify the COF ammonia (NH_4OH) was used. To test adsorption, U(VI) stock solution was prepared from uranyl nitrate hexahydrate ($UO_2(NO_3)_2{\cdot}6H_2O$, ≥99.8%, Sigma-Aldrich) was used and for desorption, HNO_3 (65%) were used.

Using instrument such as Fourier Transform Infrared Spectroscopy (FTIR), ^1H NMR and ^{13}C NMR to identify functional groups and structural form of COF before and after uranyl ion adsorption. Instrument Powder X-ray Diffraction (PXRD) were used to examine the crystal structure of COF before and after uranyl ion adsorption. Scanning Electron Microscope – Energy Dispersive X-Ray Spectroscopy (SEM-EDX) were used to examine the surface morphology. To calculate the surface area and pore size of COF we use instrument such as BET. And to examine the surface charge characteristics of COF before and after uranyl ion adsorption instrument such as Zeta Potential were used.

COF Synthesis and Ammoniation Modification COF Synthesis

The synthesis of COF using the Dissolution-Precipitation (DP) method, involves reacting an aldehyde and an amine in water in the presence of imidazole, followed by precipitation with methanol [4]. However, in a previous study, it was explained that the use of alcohol for precipitation can influence the characteristic of COF, specifically in terms of morphology, crystallinity, surface area, and the distribution of sulfonate groups, thereby affecting uranium adsorption performance [5]. The study demonstrated that the COF achieved using isopropanol as the precipitant was superior to that achieved with other alcohols (methanol, ethanol, and butanol) therefore, this study will use the optimal precipitant, namely isopropanol [5].

A total of 0.0662 grams of 2,4,6-triformylphloroglucinol (0.0003 mol), 0.0587 grams of 2,5-diaminobenzenesulfonic acid (0.0003 mol), and 0.1504 grams of imidazole were mixed in a 100-mL beaker containing 10 mL of distilled water. The mixture was stirred for 15 minutes, then 50 mL of isopropanol was added the resulting precipitate was allowed to rest for 24 hours. The solid and solution then centrifuged for 15 minutes to obtain the maximum amount of solid, followed by decantation to leave only the solid. The solid is then washed by adding DMF, water, and methanol. Before transferring to the next solution, it is centrifuged for 10 minutes to ensure thorough washing, then dried in a vacuum oven at 80°C until completely dry. The dried solid was ground to obtain a black powder consisting of COF free of impurities with molar yield of ~91%. From now on, this sample will be referred as COF IPA Non-Ammoniating.

Ammoniation Modification

Using the ammoniation method from the previous study, 50 milligrams of COF were added to a 25-ml beaker, followed by 10 ml of 1% NH_4OH [3]. The mixture was then stirred for 30 hours. Before decanting, centrifugation is performed to obtain the maximum amount of solid, then the mixture is decanted to yield ammonium COF in the form of a reddish-black powder. It is then washed with distilled water and methanol, with centrifugation performed between each wash for 15 minutes. Finally, it is dried in a vacuum oven at 80°C until dry and then the dried solid was ground to obtain gravimetric yield ~75%, this reduction in yield may be due to the loss of COF during washing or crushing [3]. From now on, this sample will be referred as COF IPA Ammoniating.

Adsorption behaviour of U(VI)

The adsorption test was conducted using the batch method. This experiment aims to determine the optimum contact time, maximum capacity, optimum temperature, and chemostability of COF IPA Non-Ammoniating and COF IPA Ammoniating during the adsorption of UO_2^{2+}. The uranium used was derived from uranyl nitrate hexahydrate, with an optimum pH of 5 [3], [4], [5], [7], [8], [9] adjusted using NaOH and HNO_3. The adsorption capacity (q_e) (mg/g) can then be calculated using the Equation (1).

$$q_e = \frac{V(C_0 - C_e)}{M} \quad (1)$$

Whereas C_0 is the initial concentration (mg/L), C_e is the equilibrium concentration of

uranyl ion (mg/L), V is the volume of solution sample (L) and for M is for amount of used adsorbent in the adsorption experiment (g). For the percentage of adsorption of uranyl ion can be calculated using Equation (2).

$$Adsorption\ \% = \left(\frac{(C_0 - C_e)}{C_0}\right) x\ 100 \qquad (2)$$

Kinetic Adsorption

Kinetic studies were conducted using 20 mL of a 300 mg/L U(VI) solution, which was then added to a beaker containing 10 mg of COF IPA (both the ammoniated and non-ammoniated forms). Contact times were varied to 15, 30, 60, 120, 240, and 1,440 minutes. Afterward, the COFs were separated from the solutions, and the solutions were analysed using an Arsenazo (III) complexing agent for analysis via UV-Vis spectroscopy [10].

Isotherm Adsorption

The adsorption isotherm test was conducted by preparing 20 mL U(VI) solution at pH 5 with varying concentrations namely, 50, 100, 300, 500, 800, and 1000 mg/L and placing them in beakers. Then, 10 mg of both the ammoniated and non-ammoniated COF IPA was added to each concentration. The mixtures were stirred for 24 hours. Afterward, the COFs were separated from the solutions, and the solutions were analysed using an Arsenazo (III) complexing agent for analysis via UV-Vis spectroscopy [10].

Thermodynamic

The thermodynamic test was conducted using 20 mL of a uranium solution with a pH of 5 and a concentration of 300 mg/L, which was placed in beakers at various temperatures: 274.15, 299.15, 313.15, 323.15, 333.15, 353.15 K. Then, 20 mg of COFs was added to each beaker. The mixtures were stirred for 2 hours. Afterward, the COFs were separated from the solutions, and the solutions were analysed using an Arsenazo (III) complexing agent for analysis via UV-Vis spectroscopy [10].

Chemostability

In the chemostability test, 20 mg of COF IPA Ammoniating was used. The procedure began with adsorption: COF IPA Ammoniating was placed in a beaker, followed by the addition of a 20mL of 200 mg/L U(VI) solution at pH 5, which was then stirred for 1 hour. After 1 hour, the COF was separated from the solution, and the solution was then analysed. Next, the uranium in the COF was desorbed by adding 20 mL of 1 M HNO_3, followed by stirring for 30 minutes. After 30 minutes, the COF was separated from the uranyl solution, and the solution was then analysed. This test was performed over four adsorption-desorption cycles.

RESULTS AND DISCUSSION

Synthesis COFSO_3H via DP Method

In this imine-based COF synthesis, the Schiff base condensation reaction is used a reaction that employs aldehydes and amines as precursors. This reaction produces an imine-bonded COF and water. The aldehyde used is 2,4,6-triformylphloroglucinol, and the amine used is 2,5-diaminobenzenesulfonic acid. To facilitate the reaction between the precursors, an imidazole base is used as a catalyst. This is because imidazole acts as both a hydrogen donor and acceptor and exhibits weak acidity in water. Thus, imidazole can deprotonate the ammonium ion (NH_3^+) to revert to an amine (NH_2), allowing nucleophilic attack on the carbonyl carbon of the aldehyde by the nitrogen atom of the amine to occur [4], [5]. The dissolution-precipitation synthesis method consists of two stages: the first stage is dissolution, and the second stage is precipitation. The detailed reaction mechanism is described in the study [5].

From the Figure 1 spectrum, the characterization results can be analysed, such as the formation of a (C=O) at a wavenumber of 1570 cm^{-1}, which originates from the β-ketoenamine bond that forms in place of the (C=O) bond of the aldehyde, and the shift of the (N-H) wavenumber to 3600–3790 cm^{-1}. Furthermore, a (C=C) was observed at a wavenumber of 1431 cm^{-1}, along with the formation of a new (C-N) at a wavenumber of 1215 cm^{-1}. Meanwhile, the sulfonate groups in the COF material appear in the wavenumber range of 1010–1095 cm [3], [4], [5], [11], [12].

After the COF was formed, characterization was performed using PXRD

 DOI: https://doi.org/10.55981/urania.2026.17361

to evaluate the structural and crystallinity of the synthesized COF. The Figure 2 shows that the COF, after synthesis, exhibits a peak at 2θ = 26.441°, corresponding to the (001) plane, which indicates π–π interlayer stacking within the COF, and a peak at 2θ = 5.04°, corresponding to the (110) plane, which indicates in-plane periodicity [4], [5], [13], [14], [15], [16], [17], [18] .The *d* spacing at the 26.441 peak is 3.37 Å (0.337 nm), while at the 5.04 peak, the *d* spacing is 17.51 Å (1.751 nm).

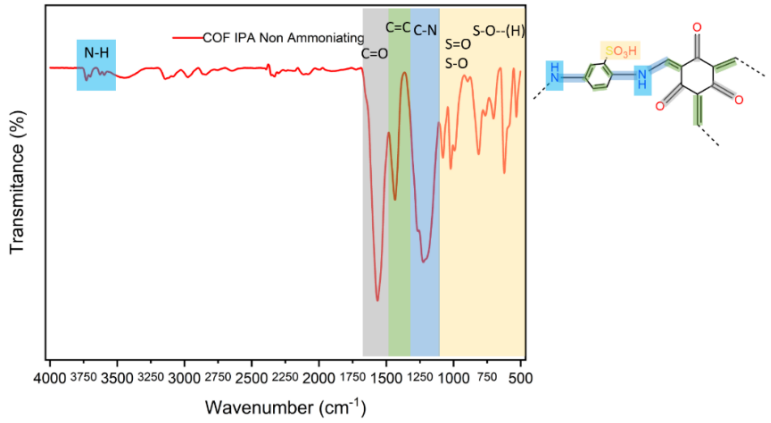

Figure 1. FTIR Characterization $COFSO_3H$.

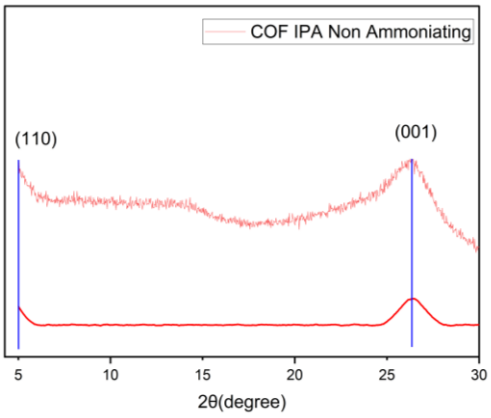

Figure 2. XRD Characterization $COFSO_3H$.

From the ^1H NMR spectrum shown at Figure 3, several major signals were observed at δ 8.20, 8.13, 7.95, 7.28, and 2.89 ppm. The three signals in the aromatic region (δ 8.13; 7.95; 7.28) originate from aromatic protons with different chemical environments due to the presence of the sulfonate group (-SO_3H) and the imine group (-NH-) that have formed. Furthermore, the signal indicating the formation of a COF from the Schiff base reaction can be seen from the proton signal bound to the (-NH-) group at 2.89 ppm due to the formation of the imine group; this occurs when a COF has been formed from the Schiff base reaction [4], [5].

The ^{13}C NMR spectrum shown at Figure 3 reveals four main signals at δ 163.51, 162.80, 36.27, and 31.25 ppm. The signal at δ 163.51 corresponds to C=O. This occurs because the carbon atom is subject to a deshielding effect caused by the O atom therefore, this signal can also be used to confirm the formation of a ketone bond, indicating that the synthesized COF is as intended [4], [5].

Based on the characterization results from the FTIR, ^1H NMR & ^{13}C NMR spectra and PXRD, it was confirmed that the synthesized COF corresponds to the planned $COFSO_3H$. This synthesis resulted a molar yield of ~91% this COF is designated as COF IPA Non-Ammoniating.

Ammoniation modification for $COFSO_3H$

Ammoniation of COF-SO_3H is a process in which the sulfonic acid functional group (–SO_3H) is converted to the ammonium sulfonate salt (–$SO_3^-NH_4^+$) through an acid–base reaction using an ammonium hydroxide (NH_4OH) solution. The sulfonic acid group (–SO_3H) is a strong acid because its conjugate base, the sulfonate anion (–SO_3^-), is highly stable] due to the delocalization of the negative charge on the oxygen atoms. Therefore, the -SO_3H group tends to undergo deprotonation, forming a sulfonate anion (–SO_3^-).

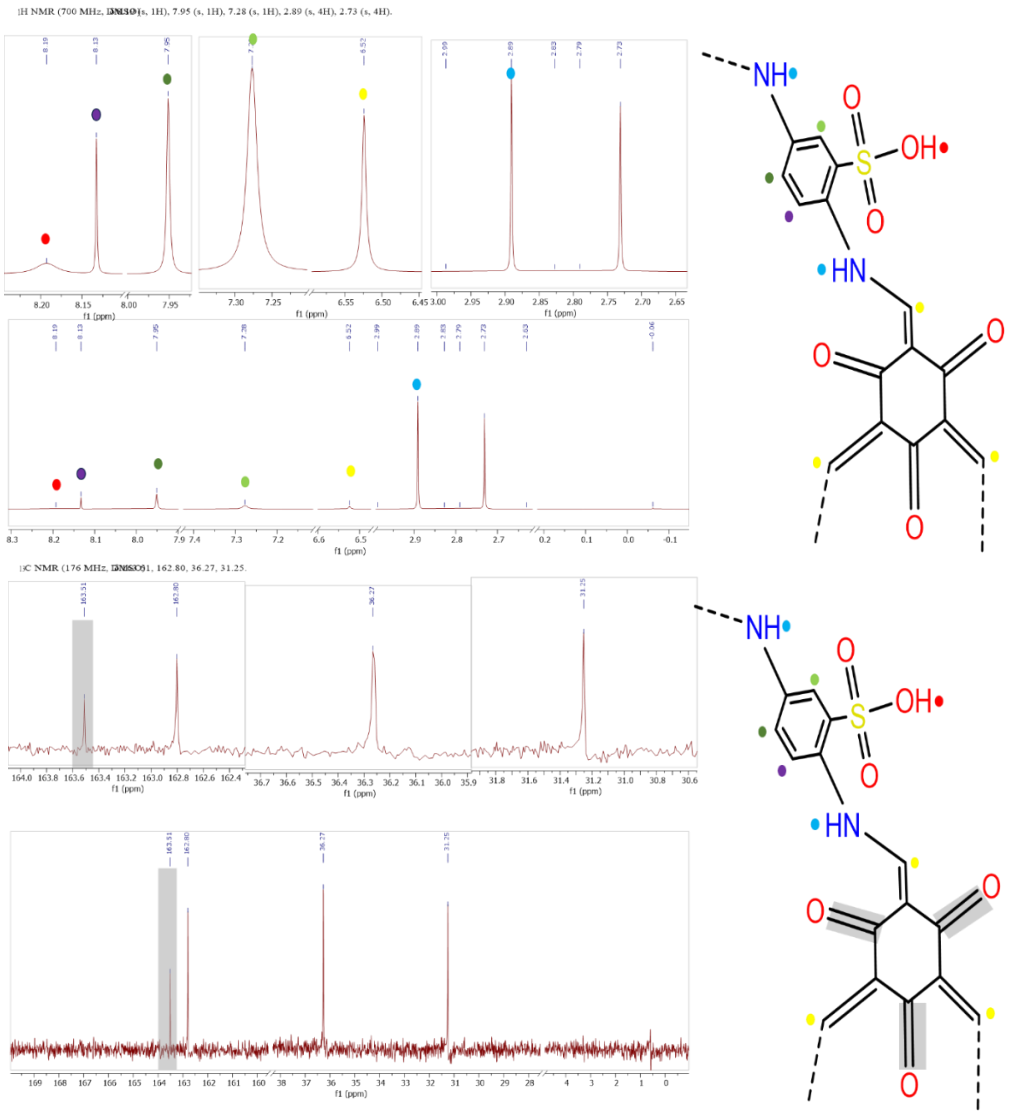

Figure 3. ^{1}H NMR & ^{13}C NMR.

Chemically, NH_4OH is a solution of ammonia (NH_3) in water that is in equilibrium with ammonium ions (NH_4^+) and hydroxide ions (OH^-), as shown Figure 4. The lone pair of electrons on the nitrogen atom of NH_3 acts as a Brønsted–Lowry base that accepts a proton from a water molecule, thereby producing NH_4^+ and OH^- ions.

The hydroxide ions formed then act as bases that deprotonate the SO_3H on the COF surface, causing the proton in the sulfonic acid group to be released and forming H_2O molecules. As a result of this deprotonation process, the SO_3H group is converted into a SO_3^-. The ammonium ion (NH_4^+), formed from the equilibrium of the NH_4OH solution, acts as a counterion for the negatively charged sulfonate. The interaction between the SO_3^- group and NH_4^+ does not result in a new covalent bond but rather forms an ion pair stabilized by the electrostatic attraction between the negative charge on the sulfonate anion and the positive charge on the ammonium ion. In addition, the hydrogen atom on the NH_4^+ ion can also form a hydrogen bond (N–H···O) with the oxygen atom in the sulfonate group. The combination of these electrostatic interactions and hydrogen bonds results in the ion pair structure of the ammonium sulfonate salt ($–SO_3^-NH_4^+$) [19].

 DOI: https://doi.org/10.55981/urania.2026.17361

The ammoniation modification of COF does not modify the primary covalent structure of the β-ketoenamine backbone rather, it forms ion pairs stabilized by electrostatic forces between the negative charge on the SO_3^- and the positive charge on the NH_4^+, resulting in ($COF–SO_3^-NH_4^+$) [19].

Therefore, ^1H NMR and ^{13}C NMR are not the key characterization methods for evaluating the success of the ammoniation process, as the expected changes primarily occur in the ionization state of the sulfonate group, rather than forming or breaking covalent bonds in the COF backbone [3], [20]. A study by Xiong et al. showed that the β-ketoenamine framework is maintained after ammoniation, while changes resulting from deprotonation and the presence of NH_4^+ can be confirmed via FTIR. These changes in the protonation state result in an increase in the fraction of negatively charged sulfonic acid groups ($–SO_3^-$), thereby altering the surface charge environment of the COF. Therefore, zeta potential analysis was used to evaluate changes in the COF surface charge before and after ammoniation modification. Thus, the COF resulting from this ammoniation modification will be called COF IPA Ammoniating. this modification yields a gravimetric yield of ~75%.

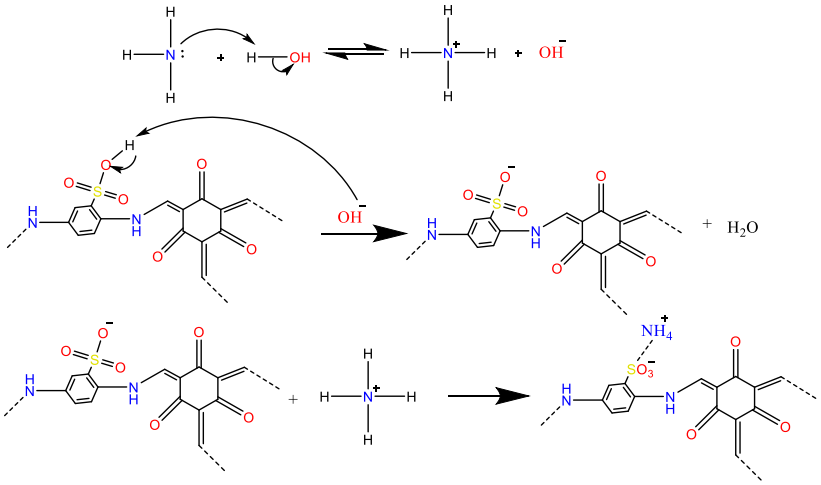

Figure 4. The reaction mechanism for the ammoniation of COF SO_3H.

Characterization of COF after modification.

Fourier Transform Infrared Spectroscopy

Characterization of COF before and after ammoniation shown at Figure 5 indicated that the β-ketoenamine framework is still maintained after ammoniation, as indicated by the insignificant change in the (C=O) band in the 1570 cm^{-1} range, also in the (C=C) band in the 1431 cm^{-1} also in the (C-N) band in the 1215 cm^{-1}, so it can be concluded that the ammoniation process does not cause changes in the main structure of COF.

Furthermore, there is an increase in the intensity of the broad band in the 3000–3300 cm^{-1} region, which is caused by the (N–H) stretching vibration of the NH_4^+ ion [21]. The main changes occurred in the sulfonate group region, namely (S=O and S-O), in the 1010–1095 cm^{-1} range, resulting in changes in intensity and a slight shift following the ammoniation modification. This is caused by changes in the electronic environment of the sulfonate groups due to the formation of the SO_3^-–NH_4^+ ion pair. These changes affect the asymmetric and symmetric stretching vibrations (O=S=O) as well as the (S–O) vibrations, which are known to be sensitive to the protonation and deprotonation of sulfonate groups. In this case, the ammoniation modification deprotonates the sulfonate, forming a sulfonate salt (SO_3-NH_4^+), which causes a shift in the bands observed in the FTIR characterization [22]. Thus, the FTIR analysis shows that the ammoniation modification successfully modified the functional groups on the COF without altering its backbone structure.

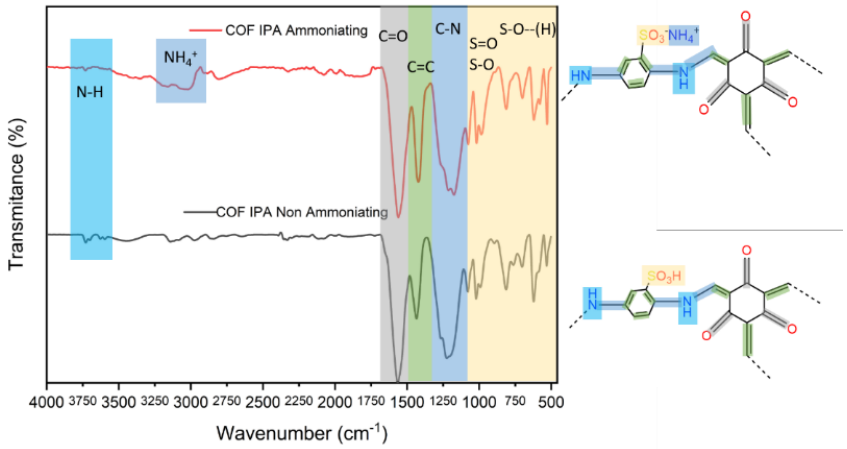

Figure 5. Characterization before and after ammoniation COF.

Scanning Electron Microscopy-Energy Dispersive Xray

From Figure 6a, the morphology of COF before ammoniation modification consists of particle aggregates with voids between the particles, indicating the presence of a porous structure in the synthesized COF material. After modification, as shown in Figure 6b, no significant morphological changes are observed, as the modification does not alter the COF's primary framework. However, there are changes in the surface morphology of the COF after ammonium modification, such as smaller interparticle pores and particles that appear more tightly packed. This may occur due to the presence of NH_4^+ on the surface of the COF [3].

EDX characterization results for COF prior to ammoniation modification show that COF consists of the elements C, N, O, and S. The presence of carbon and nitrogen confirms the formation of the COF framework resulting from the condensation between aldehyde and amine groups, which produces a β-ketoenamine structure, while the sulphur originates from the sulfonate group, indicating that the sulfonate group from the amine is preserved after the synthesis process.

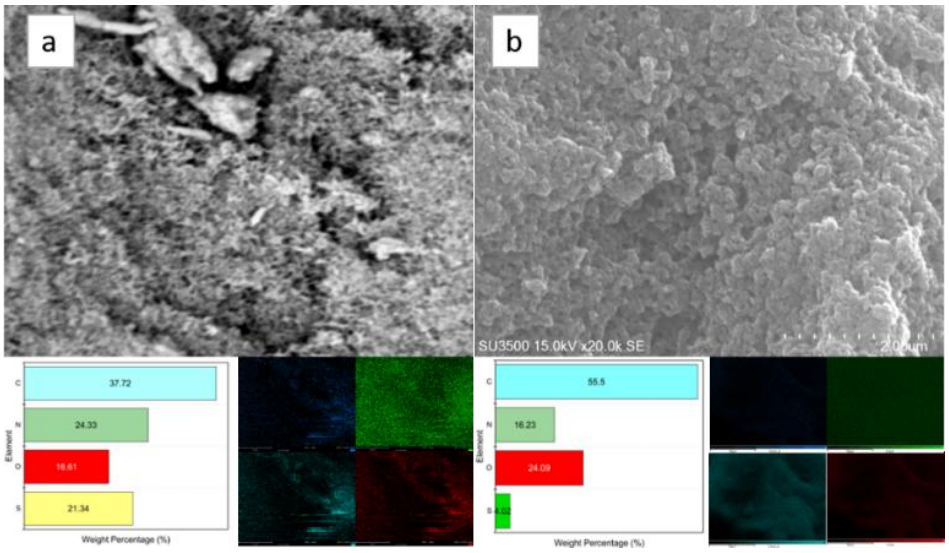

Figure 6. SEM-EDX characterization for COF IPA Non-Ammoniating (a); and COF IPA Ammoniating (b).

 DOI: https://doi.org/10.55981/urania.2026.17361

Powder X-ray Diffraction

After the COF went through the ammoniation process, XRD characterization results shown in Figure 7 indicated that, after the ammoniation process, the COF was able to retain its main diffraction peaks, namely the 2θ = 5 and 26.4 peaks. Although there was a slight shift from 5.04 and 26.414 to 5 and 26.391, this was likely due to the ammoniation process altering the 26.411° (π–π interlayer) and 5.04° (in-plane periodicity) angles in COF [3]. Furthermore, the d-spacing at the 26.391 peak is 3.37 Å (0.337 nm), while at the 5.04 peak, the d-spacing is 17.50 Å (1.750 nm). It can therefore be concluded that this ammoniation modification does not affect the main framework of COF by not altering the covalent bonds, so that the preserved main structure can be detected by XRD.

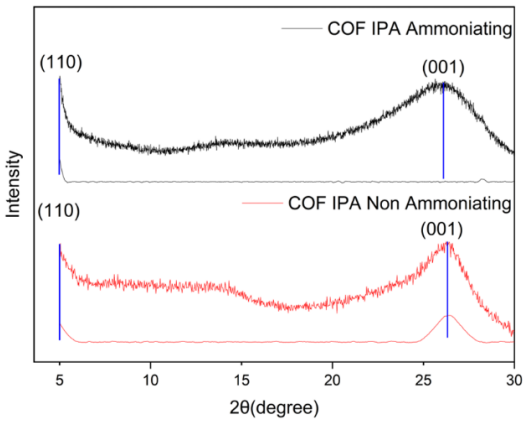

Figure 7. Characterization before and after ammoniation COF

Brunauer–Emmett–Teller

The results of the N_2 gas adsorption/desorption curves for the samples, analysed using the Brunauer–Emmett–Teller (BET) method, shown at Figure 8 indicate that these isotherm curves are of Type IV, indicating that COF before and after ammoniation possesses a mesoporous structure (2–50 nm) [23]. From the Figure 8, it can also be seen that the pore structure of the COF before and after ammoniation can be assumed to remain intact. Furthermore, the amount of adsorbed nitrogen before and after the ammoniation modification decreased from 190 cm^3/g STP to 75 cm^3/g STP. This indicates that the ammoniation modification reduces the accessibility of the pores to nitrogen molecules. This is because the ammoniation modification forms SO_3^--NH_4^+ ion pairs on the internal pore surface, causing part of the pore space to become occupied, so that nitrogen can no longer access the entire internal surface of the material [3].

From Table 1, it is shown that the ammoniation affects the BET measurements. This can be seen from the decrease in the Specific Surface Area and Pore Volume values, as well as the increase in the Pore Size value. The decrease in the Specific Surface Area value may be due to changes in the COF main framework environment following an ammoniation. The formation of NH_4^+ on the main framework can increase the mass per unit of structure, while the presence of ionic groups or species on the main framework can also reduce the accessibility of the internal surface and pore spaces to N_2 molecules during BET measurements. This phenomenon was also observed in a study by Hussain et al [20]. Thus, the decrease in SSA following ammoniation modification in this study is likely the result of a combination of changes in mass per unit structure and reduced surface/pore accessibility after modification. This was also observed during pore volume measurements, which showed a decrease following ammonium modification, indicating an increase in mass per unit and reduced pore space accessibility due to the presence of NH_4^+ in the sulfonate group environment. However, there was an increase in the pore size value following ammonium modification. This phenomenon differs from the findings in the study by Xiong et al., while this does not directly indicate that ammonium modification causes physical enlargement of COF pores, it is suspected that changes in pore distribution and accessibility occur following the modification [3].

Table 1. Results of the analysis using the Brunauer–Emmett–Teller method.

COFs	Specific Surface Area (m^2/g)	Pore Volume (cc/g)	Pore Size (nm)
COF IPA Non-Ammoniating	36.75	0.2884	15.17
COF IPA Ammoniating	11.88	0.1155	38.12

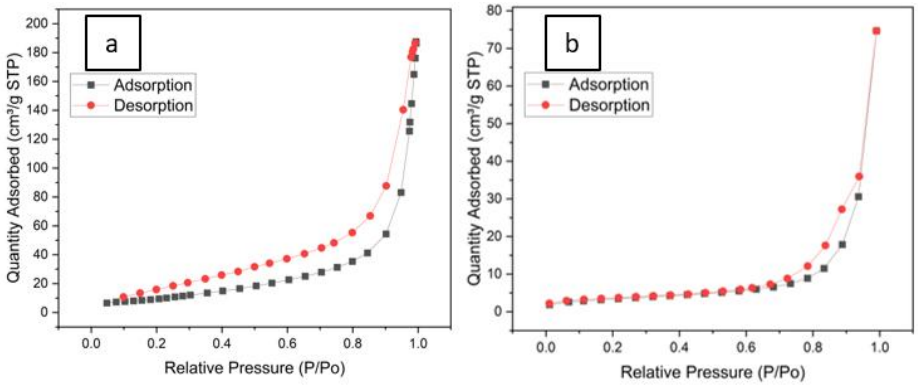

Figure 8. N2 Adsorption/desorption isotherm COF before ammoniation modification (a); and N2 Adsorption/desorption isotherm COF after ammoniation modification (b).

Zeta Potential

The results of the zeta potential characterization shown at Figure 9, the result shown a change in value from −47.4 mV for COF IPA Non-Ammoniating to −58.3 mV for COF IPA Ammoniating, indicating that the COF surface became more negatively charged. This change is related to the deprotonation of the $–SO_3H$ group to $–SO_3^-$ during ammoniation, while NH_4^+ acts as a counterion through electrostatic interactions and hydrogen bonding without neutralizing the entire negative charge of the sulfonate [21].

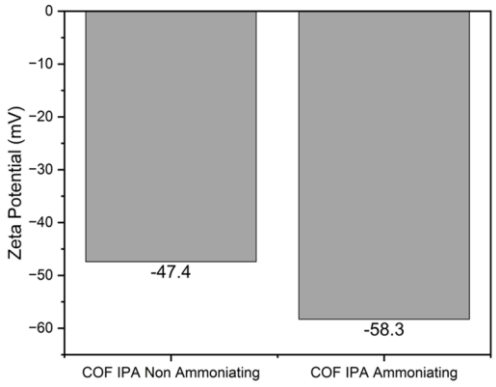

Figure 9. Zeta Potential for both COFs.

The increase in the $–SO_3^-$ fraction causes the effective negative charge on the slipping plane to become more dominant, resulting in a more negative zeta potential value [26]. Both COFs have zeta potential values < −30 mV, classifying them as strongly anionic materials with the potential to enhance electrostatic interactions with UO_2^{2+} cationic species. furthermore, the COF IPA Ammoniating has a more negative zeta potential, thereby maximizing the effective surface area for U(VI) adsorption.

Characterization of the COF after U(VI) adsorption

Scanning Electron Microscopy

SEM–characterization of COFs after U(VI) adsorption shown at Figure 10 revealed a surface morphology identical to that before adsorption. However, the BSE images showed several areas with higher brightness, indicating the presence of species with relatively high atomic numbers. BSE images reveal compositional contrast based on the atomic number of the elements present in the sample. This atomic number contrast is extremely valuable for detecting elements in samples with a variety of chemical compositions. Elements with higher atomic numbers appear brighter in BSE images, while those with lower atomic numbers appear darker [24]. Since uranium has a higher atomic number than other elements, it appears brighter than the others [25].

Fourier Transform Infrared Spectroscopy

The FTIR results after adsorption of both samples showed in Figure 11 shown changes in several peaks, particularly in the region corresponding to the sulfonate groups on both adsorbents. This indicates that the sulfonate groups ($-SO_3^-$) form coordinate bonds with UO_2^{2+}. Consequently, the peak shift at 921 cm^{-1} results from S-O-U interactions. This causes a shift in the peak range of the sulfonate groups (1010–1095 cm^{-1}) [5], [26], [27], [28]. Furthermore,

 DOI: https://doi.org/10.55981/urania.2026.17361

during the adsorption of uranium on COF IPA Ammoniating, a reduction in the NH_4^+ vibrational peak (3000–3300 cm^{-1}) occurs. This indicates that ion exchange takes place between NH_4^+ and UO_2^{2+} [3]. Both COFs itself are still able to retain its chemical structure, as evidenced by the presence of the main peaks: C=C (1431 cm^{-1}), C=O (1570 cm^{-1}), N-H (3600–3790 cm^{-1}), and C-N (1215 cm^{-1}). Therefore, it can be concluded that the adsorption of uranium ions affects the environment of the sulfonate group ($-SO_3^-$).

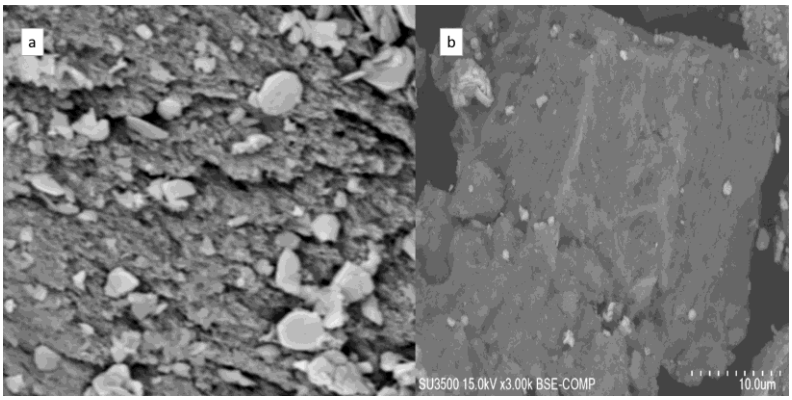

Figure 10. SEM characterization after adsorption Uranium for COF IPA Non-Ammoniating (a); and COF IPA Ammoniating (b).

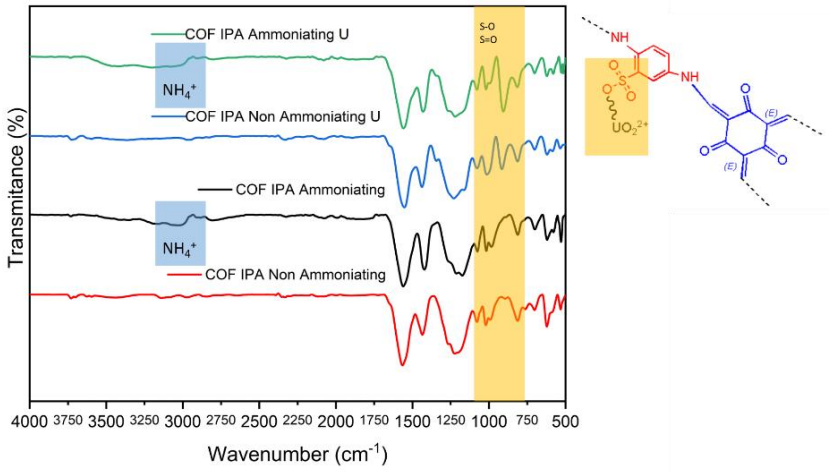

Figure 11. FTIR after U(VI) adsorption.

Powder X-ray Diffraction

After adsorption, changes in both COF characterization peaks were observed using XRD the result shown at Figure 12, after adsorption there is a decrease in the intensity of the peak at 2θ = 5.04° and at 2θ = 26.441° for both of COFs [3], [29]. This was due to the incorporation of UO_2^{2+} into the COF crystal structure, as evidenced by the formation of a new peak at 2θ = 12.084°on both COFs, However, in the COF IPA Ammoniating, new peaks are observed at 2θ = 23.052°, 25.130°, and 27.60°. These peaks may result from the formation of ammonium uranate (ADU).

Zeta Potential

In the characterization of the zeta potential after U(VI) adsorption shown in Figure 13, a change in surface charge was observed in both COFs: in the non-ammoniated IPA COF, the zeta potential decreased from -47.4 to -41.7 mV, while in the ammoniated IPA COF, it decreased from -58.3 to -44.5 mV. This indicates the presence of an interaction between the $-SO_3^-$

group and UO_2^{2+}. The interaction takes the form of electrostatic attraction, ion exchange, and coordination bonding with oxygen atoms in the sulfonate group, causing the charge on the surface layer to become less negative [3].

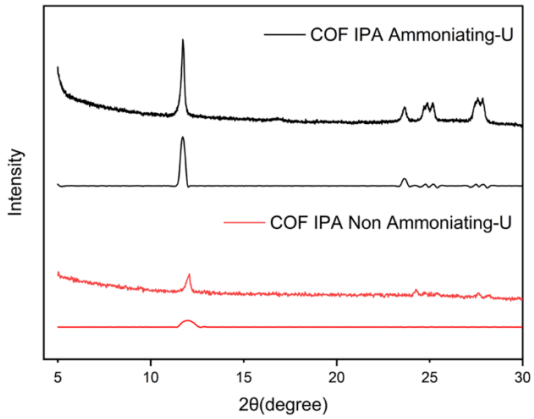

Figure 12. XRD after U(VI) adsorption.

Since the zeta potential reflects the electrical potential at the slipping plane, the presence of strong bonds between UO_2^{2+} and the SO_3^- groups indicate a characterization that does not contribute significantly to the diffuse layer and therefore has only a limited effect on the measured zeta potential [5]. The shift toward less negative zeta potential after U(VI) adsorption is consistent with partial charge compensation associated with U(VI) interaction at the COF surface.

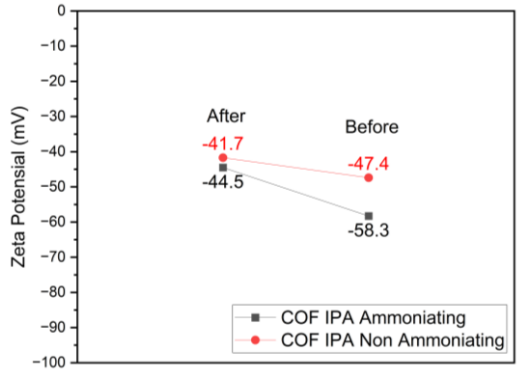

Figure 13. Zeta Potential before and after U(VI) adsorption.

Adsorption behaviour of U(VI)

Kinetics Adsorption

The results of the kinetic test are shown in the Figure 14 equilibrium is reached at 120 minutes, followed by a slight, insignificant increase from 180 minutes to 1,440 minutes. This indicates that both COF samples have an optimal time of 120 minutes as selected because subsequent increases in adsorption capacity were minimal.

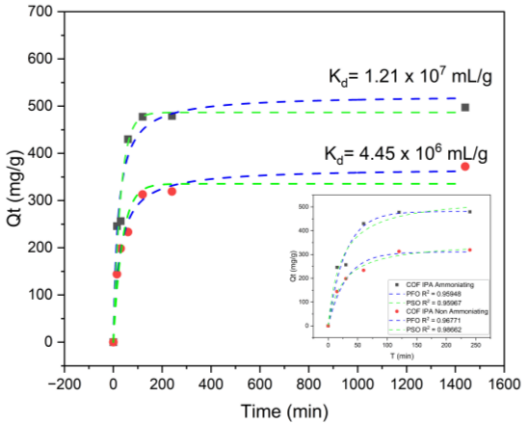

Figure 14. Kinetic Adsorption uranium for COF IPA Non-Ammoniating and COF IPA Ammoniating.

To study the effect of time on U(VI) adsorption onto COF, two common models were used to describe the interactions that occur: the pseudo-first order and pseudo-second-order models. The pseudo-first-order model is intuitively associated with the one-site-occupancy adsorption kinetics governed by the rate of surface reaction [30]. The nonlinear equation for the PFO model is written as Equation (3).

$$qt = qe(1 - e^{-k1t}) \quad (3)$$

qt is the amount of adsorbed adsorbate (mg/g) at time t (min), qe is the amount of adsorbed adsorbate per unit mass of adsorbent at equilibrium (mg/g), and k1 is rate constants of pseudo-first order (min^{-1}) [31], [32].

Meanwhile, its generalization for two-site-occupancy adsorption was proposed and termed the pseudo-second-order kinetic equation[30]. The nonlinear equation for the PSO model is written as Equation (4)

$$qt = \frac{k_2\, qe^2 t}{1 + k_2 qet} \quad (4)$$

In which qt is the amount of adsorbed adsorbate (mg/g) at time t (min), qe is the amount of adsorbed adsorbate per unit mass

 DOI: https://doi.org/10.55981/urania.2026.17361

of adsorbent at equilibrium (mg/g), and k_2 is rate constants of pseudo first order (g/mg min^{-1}) [31], [32].

The Equation (3) and Equation (4) was then used to evaluate the model's fit to the U(VI) adsorption kinetics data of the two models described above, linear and nonlinear regression. both can be used for analysis. However, in this study, the nonlinear approach was used as the primary basis for analysis. This is because the PFO and PSO equations can be directly applied to the experimental data without making mathematical changes to the variable's qt and t. This contrasts with linear regression, which requires mathematical changes to the equation. Such changes can introduce bias and uncertainty, which may lead to errors in the analysis. Therefore, the nonlinear approach has proven to be the most robust method, regardless of what type of error distribution the data may have. nonlinear regression avoids transformation of the experimental response and generally provides more appropriate parameter estimation for adsorption kinetic models [31], [33].

From the adsorption kinetics results shown at Figure 14, the PSO model is more suitable for both samples: COF IPA Non-Ammoniating results an R^2 of 0.98662, while the COF IPA Ammoniating results an R^2 of 0.95967. Therefore, the PSO model is more representative in describing the U(VI) adsorption kinetics for both samples. The kinetic parameters are presented in Table 2. The Qe values obtained from the experimental results show a 33.6% increase from the COF IPA Non-Ammoniating 372.1236 mg/g to COF IPA Ammoniating 497.3137 mg/g, indicating that the ammoniation enhances the adsorption capacity. An adsorbent with a distribution coefficient (Kd) for uranium greater than 1.0×10^4 mL/g can be considered a good adsorbent [3]. Thus, when calculating the distribution coefficient using Equation (5).

$$K_d = \frac{(C_0 - C_e)}{C_e} . \frac{V}{m} x\ 10^3 \quad (5)$$

Here, C_0 is the initial concentration of the adsorbate in the solution (mg/L), C_e is the equilibrium concentration of uranyl ion (mg/L), V is the volume of the solution (L), m is the mass of the COF adsorbent used (g), and Kd is the distribution coefficient [3] using the Equation (5), there is an increase in Kd value from 4.45×10^6 mL/g for COF IPA Non Ammoniating to 1.21×10^7 mL/g for COF IPA Ammoniating. This indicates that both COFs are good adsorbents for U(VI) adsorption [3] and that the ammoniation on the COF can enhance the affinity and distribution of uranium on the COF adsorbent.

Table 2. Kinetic Adsorption Parameter

Adsorbent	Pseudo First Order			Pseudo Second Order			Qe exp (mg/g)	KD (mL/g)
	K_1 (min^{-1})	Qe (mg/g)	R^2	K_2 (g/mg min^{-1})	Qe (mg/g)	R^2		
COF IPA Non-Ammoniating	0.0327± 0.0054	310.38 ± 15.89	0.96771	1.2 x10^{-4} ± 2.4 x10^{-5}	355.03 ± 15.80	0.98662	372.1236	4.45 x 10^6
COF IPA Ammoniating	0.0343 ± 0.0064	480.72 ± 27.37	0.95948	8.2 x10^{-5} ± 2.9 x10^{-5}	544.65 ± 41.62	0.95967	497.3137	1.21 x 10^7

Isoterm Adsorption

An isotherm defines the equilibrium relationship between the concentration of an adsorbate in the liquid phase and the corresponding amount retained on the solid surface at a constant temperature. By fitting equilibrium data to these models, crucial insights can be gained regarding the adsorption mechanisms, the ultimate adsorption capacity, and the fundamental properties of the adsorbent [34].

Adsorption isotherm testing is conducted to analyse and understand the interaction between the adsorbent and the adsorbate and to determine the maximum adsorption capacity. The maximum adsorption capacity is the maximum amount of a substance (adsorbate) that can be absorbed by the adsorbent. To model the interaction between the adsorbate and the adsorbent, there are two common models: the Langmuir and Freundlich models shown at Figure 15.

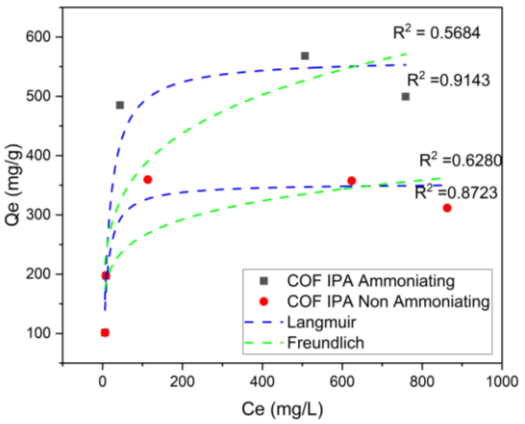

Figure 15. Isotherm Adsorption uranium for COF IPA Non-Ammoniating and COF IPA Ammoniating.

The Langmuir model makes four assumptions: (1) monolayer adsorption; (2) the distribution of adsorption sites is homogeneous; (3) the adsorption energy is constant; and (4) the interaction between adsorbate molecules is negligible [34]. The nonlinear equation of the Langmuir model is as Equation (6)

$$q_e = \frac{q_m K_L C_e}{1 + K_L C_e} \; [35] \qquad (6)$$

In which q_e is the amount of adsorbed adsorbate per unit mass of adsorbent at equilibrium (mg/g), q_m is the maximum monolayer adsorption capacity (mg/g), K_L is the Langmuir constant (L/mg), and C_e is the concentration of the adsorbate in the solution at equilibrium (mg/L).

In this study, calculations for the Langmuir model will be performed using a nonlinear method. This is because calculations using a linear method produce inaccurate results and introduce bias [36]; therefore, the nonlinear method is preferable for determining the Langmuir parameters to avoid the drawback of the linear method [37]. In addition, there is a common dimensionless constant called the separation factor (R_L) written as Equation (7)[38].

$$R_L = \frac{1}{1 + K_L C_0} \; [38] \qquad (7)$$

Thus, the results of the calculation of the separation factor RI can be explained as follows: if RI > 1, RI = 1, and RI < 1, these values indicate, respectively, that the adsorption is unfavorable, linear, and favorable [38].

The second model is the Freundlich model. The Freundlich model is an empirical model that shows that adsorption does not occur uniformly across the entire adsorbent (heterogeneous) and that the adsorption process allows for the formation of multiple layers, with interactions occurring between adjacent adsorbed molecules [39]. The nonlinear equation written as Equation (8).

$$q_e = K_f C_e^{1/n} \; [40] \qquad (8)$$

Whereas qe is the amount of adsorbed adsorbate per unit mass of adsorbent at equilibrium (mg/g), Ce is the concentration of the adsorbate in the solution at equilibrium (mg/L), and KF is the Freundlich constant related to the adsorption capacity (mg/g). n is the surface heterogeneity factor constant.

Just like the Langmuir model, the Freundlich model in this study will use a nonlinear basis. This is because a linear basis would result in propagated errors, which lead to inaccurate parameter estimates [36]. The parameters of the Langmuir and Freundlich models are presented in Table 3. It can be seen from Figure 15 and Table 3, that the Langmuir model provides a better fit than the Freundlich model for both adsorbents, as indicated by R^2 values of 0.8723 for COF IPA Non-Ammoniating and 0.9143 for COF IPA Ammoniating. Thus, it can be assumed that the adsorption that occurs follows the Langmuir model. Furthermore, from the Langmuir model nonlinear Equation (6), the theoretical Qm was calculated to be 353.42 ± 25.72 mg/g for COF IPA Non-Ammoniating and 564.09 ± 44.61 mg/g for COF IPA Ammoniating from initial U(VI) concentrations of 50, 100, 300, 500, 800, and 1000 mg/L. From the calculated separation factor values, both adsorbents have values below 1. This indicates that the separation of uranium using the COF IPA Ammoniating and COF IPA Non-Ammoniating adsorbents are favorable [38]. Therefore, it can be said that the ammoniation can increase the adsorption capacity and efficiency for U(VI) adsorption.

 DOI: https://doi.org/10.55981/urania.2026.17361

Table 3. Isotherm Adsorption Parameter.

Adsorbent	Langmuir Model				Freundlich Model			Qe exp (mg/g)
	K_L (L/mg)	Qm (mg/g)	R^2	R_L	K_F (mg/g)	1/n	R^2	
COF IPA Non-Ammoniating	0.1093 ± 0.0403	353.42 ± 25.72	0.8723	0.0088	151.884	0.1997	0.6280	359.54175
COF IPA Ammoniating	0.0655 ± 0.0233	564.09 ± 44.61	0.9143	0.0145	133.927	0.1472	0.5684	568.22811

Thermodynamic

Thermodynamic tests were conducted to evaluate the effect of temperature on the adsorption of uranium onto COFs. This was done by evaluating thermodynamic parameters, such as the standard Gibbs free energy change (ΔG^o), enthalpy change (ΔH^o), and entropy change (ΔS^o), which were obtained from the following equations:

$$K_c = K_D . \rho_{water} = K_D . 1000\ L/g \quad (9)$$

$$\ln K_c = \left(\frac{\Delta S^o}{R}\right) - \left(\frac{\Delta H^o}{R}\right)\frac{1}{T} \quad (10)$$

$$\Delta G^o = -RT ln K_c \quad (11)$$

where ΔS^o is the change in entropy (J/mol·K), ΔG^o is the change in Gibbs free energy (kJ/mol), T is the temperature (K), ΔH^o is the change in enthalpy (kJ/mol·K), R is the gas constant of 8.314 J/(mol·K) [28], [41]. K_C is the adsorption equilibrium constant calculated from experimental data which is K_D, however K_D is a dimensional coefficient, with common unit such as L/g, therefore it needs to be dimensionless, some author [42] recommended to convert the unit of K_D (L/g) into K_c by simply multiplying K_D value by 1000 g/L since it's the solution density is approximately equal to 1000 g/L [42], [43].

The ΔH^o and ΔS^o parameters can be determined from the slope and intercept of the plot of ln Kd versus 1/T; this plot is known as the Van't Hoff plot. Then, Equation 11 is used to determine ΔG^o.

From Figure 16, two phenomena occur in COFs: when temperature is increased during adsorption, COF IPA Non-Ammoniating shows an increase in the percentage of adsorption, whereas COF IPA Ammoniating shows a decrease in the percentage of adsorption. Upon plotting the Van't Hoff plot, The COF IPA Non-Ammoniating appears linear in Figure 16, Thus, data from temperatures ranging from 274.15 to 328.15 K can be analyzed shown by Figure 17.

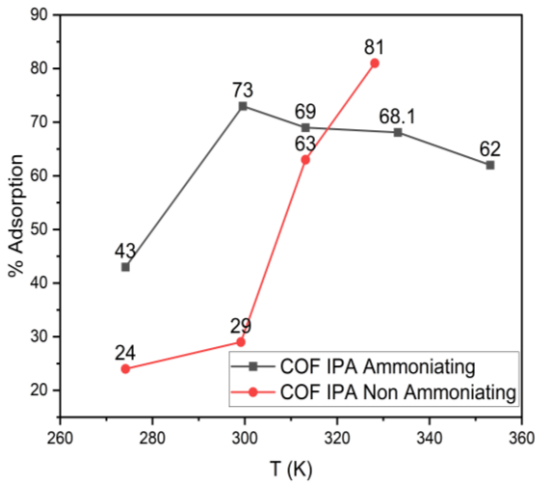

Figure 16. Effect of temperature on percentage adsorption.

The enthalpy change values can be used to distinguish between physisorption and chemisorption. ΔH^o values ranging from 2.1 to 20.9 kJ/mol (0.5 to 5 kcal/mol) indicate physisorption, while ΔH^o values ranging from 20.9 to 418.4 kJ/mol (5 to 100 kcal/mol) indicate chemisorption [32].

However, this trend cannot be directly applied to the COF IPA Ammoniating, as the COF IPA Ammoniating in Figure 16 appears nonlinear; therefore, the Van't Hoff plot can only be evaluated for temperatures ranging from 299.15 to 353.15 shown by Figure 17. Meanwhile, the temperature range from 274.15 to 299.15 consists of only two data points, so it cannot be evaluated.

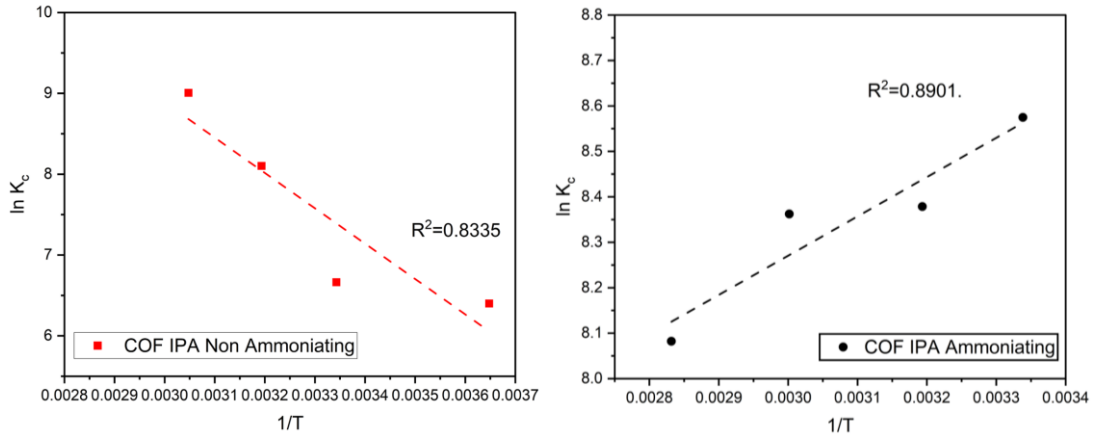

Figure 17. Vant Hoff Plot for COF IPA Non-Ammoniating and COF IPA Ammoniating.

From Table 4, COF IPA non-ammoniating shows a positive ΔH° value greater than 20.9, indicating that the adsorption process is endothermic and occurs via chemisorption, a positive entropy change ΔS° indicates an increase in disorder at the solid-liquid interface, suggesting a strong affinity between the adsorbent and U(VI) ions [30]. A negative ΔG° indicates that the reaction occurs spontaneously.

However, the results of this analysis differ from those of the COF IPA Ammoniating; the results are as shown in Table 5.

Table 4. COF IPA Non-Ammoniating Parameters.

Adsorbent	ΔH° (kJ/mol)	ΔS° (Jmol−1 K−1)	ΔG° (kJ/mol)			
			274.15 K	299.15 K	313.15 K	328.15 K
COF IPA Non-Ammoniating	36.3588	177.2212	-14.58	-16.57	-21.09	-24.57

Table 5. COF IPA Ammoniating Parameters.

Adsorbent	ΔH° (kJ/mol)	ΔS° (Jmol−1 K−1)	ΔG° (kJ/mol)				
			274.15 K	299.15 K	313.15 K	333.15 K	353.15 K
COF IPA Ammoniating	-7.1303	47.21	-16.71	-21.32	-21.81	-23.16	-23.73

However, COF IPA Ammoniating, significantly different values were obtained: a negative ΔH° smaller than 20.9, indicating that the adsorption process is exothermic and occurs via physisorption, a positive entropy change ΔS° indicates an increase in disorder at the solid-liquid interface. A negative ΔG° indicates that the reaction occurs spontaneously [28].

In Figure 16, a decrease in the percentage of adsorption of COF IPA Ammoniating is observed as the temperature increases. This may be due to two phenomena occurring simultaneously. The first phenomenon is ion exchange between NH_4^+ on the COF and uranium, whereby NH_4^+ acts as a counterion, allowing uranium to interact with the oxygen atoms in the sulfonate groups via coordination bonds. However, in the second phenomenon when the temperature is increased the NH_4^+ ions, which are in equilibrium with NH_3, may bond with uranium to form ammonium diuranate (ADU). This is caused by the accelerated movement of ions at high temperatures, which increases the frequency of inter-ionic collisions and thus triggers the formation of crystal nuclei. This means that ADU precipitation forms more rapidly as the temperature rises [44] .This causes cloudiness in the solution, leading to competition between the adsorption of uranyl ions on the COF and the ADU precipitation

 DOI: https://doi.org/10.55981/urania.2026.17361

process within the solution. Since adsorption efficiency is calculated based on the decrease in dissolved uranium concentration, the occurrence of precipitation can interfere with the determination of the actual adsorption capacity. Thus, for the COF IPA Ammoniating, optimal adsorption results were obtained at room temperature without the need to increase the temperature.

Chemostability

This testing aims to evaluate the ability of COF IPA Ammoniating to maintain its adsorption performance after repeated use. Its resistance to HNO_3 solution during the desorption process also provides information regarding the material's resistance to acidic conditions. The use of HNO_3 during desorption serves as a solution to desorb uranium from COF IPA Ammoniating. Figure 18 analysis shows that COF IPA Ammoniating maintains its adsorption performance, with only a 9% reduction after desorption using HNO_3 over four cycles. This indicates that COF IPA Ammoniating can maintain its chemical structure in acidic conditions and sustain its adsorption performance over four cycles.

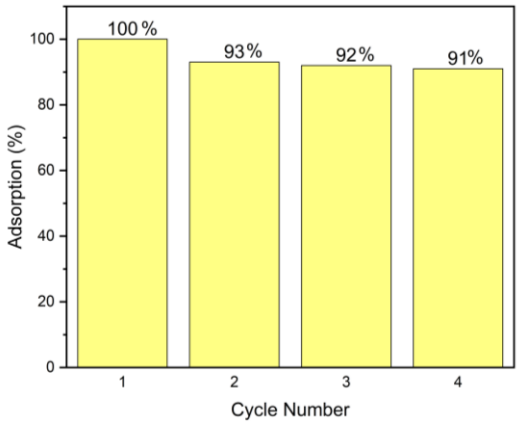

Figure 18. Chemostability of COF IPA Ammoniating.

Proposed Adsorption Mechanism of U(VI) on Ammoniated Sulfonated COFs

This ammoniation modification causes a change in the chemical environment of the COF, specifically in the vicinity of the SO_3H. Ammoniation leads to the formation of COF $SO_3^-NH_4^+$. The presence of NH_4^+ around the sulfonate groups allows for ion exchange with U(VI) species, while the $-SO_3^-$ present on the pore walls provide oxygen atoms that can interact with uranium through coordinate bonds. Thus, ammoniation results in an adsorption system with more than one binding mechanism namely, ion exchange and coordination bonding thereby increasing the affinity for uranium [3] .

Meanwhile, in COF before ammoniation, the ion exchange that occurs is between H^+ on the SO_3H with U(VI) species. This causes H^+ to be released into the uranium solution, which can cause the pH to become more acidic, thereby increasing ionic competition during uranium adsorption, which can affect the adsorption process [8]. In contrast, ammoniation converts the sulfonic acid groups into ammonium-associated sulfonate groups. Because the sulfonate groups are already in their deprotonated form, their interaction with U(VI) does not require the same proton-release process associated with the $–SO_3H$ form [3]. Furthermore, NH_4^+ may be displaced by suitable U(VI) species through ion exchange, potentially facilitating uranium retention by the sulfonate-containing framework. Although NH_4^+ is a weak acid and may have a limited effect on solution pH under certain conditions. Therefore, the enhanced U(VI) adsorption following ammoniation may be associated with the modified counterion environment, reduced dependence on proton-release equilibria, and potential ion-exchange interactions.

This can also occur according to the Hard-Soft Acid-Base (HSAB) theory, since the UO_2^{2+} species is a hard acid it has a high charge, high charge density, is highly oxophilic, acts as a strong electron acceptor, and is a member of the actinide series [45] whereas the SO_3H, which is converted into the sulfonate anion (SO_3^-), acts as a hard base due to the highly electronegative nature of its oxygen atom and its relatively small size. Thus, the sulfonate group in the form of the sulfonate anion (SO_3^-) provides an oxygen atom as an electron donor that can interact coordinatively with U(VI) [3], [46].

The zeta potential measurements provide additional evidence that ammoniation modifies the surface electrochemical properties of the COF from -47.4 mV to -58.3 mV, indicating that the surface charge became more negative. This shift toward a more negative charge can enhance electrostatic interactions with cationic uranium

species; consequently, the electrostatic interactions between the COF and uranium also help increase adsorption capacity through ion exchange and coordination bonding mechanisms involving the sulfonate groups. This combined mechanism is the primary factor responsible for the high affinity for uranium [3].

CONCLUSIONS

COF with a sulfonate group (SO_3H) was successfully synthesized using the dissolution-precipitation (DP) method, which molar yielded ~91%; this was followed by an ammoniation using 1% NH_4OH, which gravimetric yielded 75%. Characterization results from FTIR, ^{1}H NMR, ^{13}C NMR, PXRD, and SEM-EDX indicate that ammoniation did not alter the main COF framework but only modified the environment surrounding the sulfonate groups. Zeta potential results also showed an increase in value from -47.4 to -58.3 mV. The detection of ammonium species after ammoniation supports the conclusion that the environment of the sulfonate groups has been modified by ammonium.

U(VI) adsorption testing showed that the ammoniation can improve the performance of COF. Based on the nonlinear regression model, the Pseudo Second Order model was the best fit for the kinetic model, and the Langmuir model was the best fit for the isotherm model. The maximum theoretical adsorption capacity increased from 353.42 ± 25.72 to 564.09 ± 44.61 mg/g from initial U(VI) concentrations of 50, 100, 300, 500, 800, and 1000 mg/L after the ammoniation. There was also an increase in the K_D value from 4.45×10^6 to 1.21×10^7 after the ammoniating, indicating a high affinity for uranium. COF IPA Ammoniating achieved the highest adsorption at room temperature, after which the adsorption percentage decreased as the temperature increased. In contrast, COF IPA Non-Ammoniating exhibited increased adsorption as the temperature rose within the test range. Thus, based on the test conditions, COF IPA Ammoniating achieved high adsorption performance at room temperature without the need for further heating. The COF IPA Ammoniating chemostability test showed that it could maintain its adsorption performance after four adsorption-desorption cycles with a 9% decrease in performance. This increased adsorption performance for U(VI) is due to ion exchange between NH_4^+ and uranyl ions and the coordination bond between the oxygen atom in the SO_3^- group and the uranyl ion. Overall, the results demonstrate that the ammoniation can improve the adsorption performance of the COF toward U(VI).

ACKNOWLEDGEMENT

The authors would like to express sincere gratitude to the Department of Chemistry, Faculty of Mathematics and Natural Sciences, Padang State University, as well as to the Coordinator of the Nuclear Fuel Technology Research Group, the Head of the Research Center for Nuclear Fuel Technology and Radioactive Waste (PRTBNLR), the Nuclear Energy Research Organization (ORTN), and the National Research and Innovation Agency (BRIN). This research was supported by research facilities, scientific resources, and technical assistance from the Advanced Chemical Characterization Laboratory, the Nuclear Characterization Laboratory, and the Nuclear Fuel Division (DPFK) at the National Research and Innovation Agency. The authors would like to thank all those who have supported this research. The authors also hope that this research will be useful for the development of uranium separation methods for nuclear fuel.

AUTHOR CONTRIBUTION

Conceptualization: R. M. and A. S.; Methodology: R. M., E. N., M. S. and A. S.; Validation: E. N., M. S., D. M. and A. S.; Formal analysis: R. M., A. P., F. P. D., A. A. Z., M. S. A., A. A. P., S. I., R. A., M. S., D. M., E. N. and A. S.; Investigation: R. M., E. N. and A. S.; Data curation: R. M.; Writing – original draft: R. M.; Writing – review and editing: R. M., D. M., E. N. and A. S.; Visualization: R. M. and A. S.; Supervision: E. N. and A. S.; Funding acquisition: M. S.

FUNDING STATEMENT

This work was supported by National Research and Innovation Agency (BRIN) for its invaluable assistance through the 2026 Nuclear Technology Innovation Program [CFJRC-ORTN2026-2687539830045].

COMPETING INTEREST

The authors declare that they have no financial or non-financial competing interests relevant to this work.

AI USAGE DECLARATION

During the preparation of this work, the authors used Open AI ChatGPT, Deepseek and Copilot to improve the work's readability and language. After using this tool/service, the authors reviewed and edited the content as needed and took full responsibility for the publication's content.

REFERENCES

[1] A. Ardiansyah, K. Dian Meila, and P. Gantine Lestari, "Efektivitas penerapan green transition dan kebijakan karbon pada sektor energi: Literature review," *Jurnal Riset Akutansi Mercubuana*, vol. 10, Nov. 2024, doi: doi.org/10.26486/jramb.v10i2.4590.

[2] T. Gibon and Á. Hahn Menacho, "Parametric Life Cycle Assessment of Nuclear Power for Simplified Models," *Environ. Sci. Technol.*, vol. 57, no. 38, pp. 14194–14205, Sep. 2023, doi: 10.1021/acs.est.3c03190.

[3] X. H. Xiong *et al.*, "Ammoniating covalent organic framework (COF) for high-performance and selective extraction of toxic and radioactive uranium ions," *Advanced Science*, vol. 6, no. 16, Aug. 2019, doi: 10.1002/advs.201900547.

[4] L. Guo, Q. Y. Zhang, Z. Yu, R. Krishna, and F. Luo, "Minute and large-scale synthesis of covalent-organic frameworks in water at room temperature by a two-step dissolution-precipitation method," *Chemistry of Materials*, vol. 35, no. 14, pp. 5648–5656, Jul. 2023, doi: 10.1021/acs.chemmater.3c01220.

[5] A. Saputra *et al.*, "Optimizing covalent organic frameworks properties for uranium uptake: The role of alcohol in aqueous precipitation," *Appl. Mater. Today*, vol. 51, p. 103328, Aug. 2026, doi: 10.1016/j.apmt.2026.103328.

[6] D. Liu, Y. Wang, L. Zuo, M. Guo, and S. Liu, "Advanced materials for uranium adsorption: a mini review of recent developments," 2025, *Frontiers Media SA*. doi: 10.3389/fmats.2025.1541204.

[7] W. Yao, G. Zhou, T. Liu, Y. Yuan, H. Wang, and N. Wang, "Defect Engineering Activates Pyrene-Based Covalent Organic Frameworks for Efficient Photocatalytic Uranium Capture," *Advanced Science*, vol. 13, no. 11, Feb. 2026, doi: 10.1002/advs.202518948.

[8] S. Zhang, X. Li, X. Huang, M. Szlachta, H. Bao, and J. Xu, "Highly selective uranium separation using sulfonic acid-functionalized hierarchically porous zirconium phosphate: Modelling and mechanism study," *Materials Science and Engineering: B*, vol. 319, Sep. 2025, doi: 10.1016/j.mseb.2025.118342.

[9] R. Zhang *et al.*, "Sulfonated heteroatom co-doped carbon materials with a porous structure boosting electrosorption capacity for uranium (VI) removal," *J. Solid State Chem.*, vol. 327, Nov. 2023, doi: 10.1016/j.jssc.2023.124262.

[10] H. Golmohammadi, A. Rashidi, and S. J. Safdari, "Simple and rapid spectrophotometric method for determination of uranium (VI) in low grade uranium ores using arsenazo (III)," *Chemistry and Chemical Technology,* vol. 6 no. 3, pp. 245-249, 2012.

[11] B. Hao, Z. Jiang, A. Livingston, and K. Li, "High-performance COF membranes prepared by an in-situ interfacial polymerization for effective pharmaceutical fractionation," *J. Memb. Sci.*, vol. 746, Apr. 2026, doi: 10.1016/j.memsci.2026.125285.

[12] S. Chandra, T. Kundu, K. Dey, M. Addicoat, T. Heine, and R. Banerjee, "Interplaying Intrinsic and Extrinsic Proton Conductivities in Covalent Organic Frameworks," *Chemistry of Materials*, vol. 28, no. 5, pp. 1489–1494, Mar. 2016, doi: 10.1021/acs.chemmater.5b04947.

[13] S. Van Gele, S. Bette, and B. V. Lotsch, "The Devil Is in the Details: Pitfalls and Ambiguities in the Analysis of X-ray Powder Diffraction Data of 2D Covalent Organic Frameworks," *JACS Au*, vol. 5, no. 1, pp. 388–398, Jan. 2025, doi: 10.1021/jacsau.4c00979.

[14] J. Yang *et al.*, "Modulating π-bridge in donor-π-acceptor covalent organic frameworks for low-energy-light-driven

photocatalytic reaction," *J. Colloid Interface Sci.*, vol. 683, pp. 612–621, Apr. 2025, doi: 10.1016/j.jcis.2024.12.203.

[15] B. P. Biswal, S. Chandra, S. Kandambeth, B. Lukose, T. Heine, and R. Banerjee, "Mechanochemical synthesis of chemically stable isoreticular covalent organic frameworks," *J. Am. Chem. Soc.*, vol. 135, no. 14, pp. 5328–5331, Apr. 2013, doi: 10.1021/ja4017842.

[16] S. Dalapati, S. Jin, J. Gao, Y. Xu, A. Nagai, and D. Jiang, "An Azine-linked Covalent Organic Framework," 2013. [Online]. Available: http://pubs.acs.org

[17] R. Guo, Y. Liu, Y. Huo, A. Zhang, J. Hong, and Y. Ai, "Chelating effect between uranyl and pyridine N containing covalent organic frameworks A combined experimental and DFT approach," *J. Colloid Interface Sci.*, vol. Volume 606, Part 2, pp. 1617–1626, 2022, doi: https://doi.org/10.1016/j.jcis.2021.08.118.

[18] B. Zhang *et al.*, "A recyclable sulfonic covalent organic framework catalyst for enhanced activity and selectivity in HMF biorefining," *Molecular Catalysis*, vol. 603, Oct. 2026, doi: 10.1016/j.mcat.2026.116291.

[19] I. V. Fedorova and L. P. Safonova, "Influence of the dielectric constant on ion pair formation in sulfonic acid-ammonia and alkylamine systems: a CPCM-based quantum chemical study," *J. Mol. Liq.*, vol. 437, Nov. 2025, doi: 10.1016/j.molliq.2025.128288.

[20] M. Hussain, I. Ullah, S. Kumaravel, B. Kim, and D. S. Lee, "Boosting Iodine Capture via Ammonization of a Multicomponent-Based Covalent Organic Framework," *Int. J. Energy Res.*, vol. 2026, no. 1, 2026, doi: 10.1155/er/9008510.

[21] S. Petit, D. Righi, and J. Madejová, "Infrared spectroscopy of NH4+-bearing and saturated clay minerals: A review of the study of layer charge," *Appl. Clay Sci.*, vol. 34, no. 1–4, pp. 22–30, Oct. 2006, doi: 10.1016/j.clay.2006.02.007.

[22] O. L. Gribkova, V. A. Kabanova, E. I. Rodina, M. A. Teplonogova, L. I. Demina, and A. A. Nekrasov, "Optical Ammonia Sensors Based on Spray-Coated Polyaniline Complexes with Polysulfonic Acids," *Sensors*, vol. 25, no. 11, Jun. 2025, doi: 10.3390/s25113348.

[23] M. Naderi, "Surface Area: Brunauer-Emmett-Teller (BET)," in *Progress in Filtration and Separation*, Elsevier Ltd, 2015, pp. 585–608. doi: 10.1016/B978-0-12-384746-1.00014-8.

[24] A. Ali, N. Zhang, and R. M. Santos, "Mineral Characterization Using Scanning Electron Microscopy (SEM): A Review of the Fundamentals, Advancements, and Research Directions," Dec. 01, 2023, *Multidisciplinary Digital Publishing Institute (MDPI)*. doi: 10.3390/app132312600.

[25] A. C. Keatley, T. B. Scott, S. Davis, C. P. Jones, and P. Turner, "An investigation into heterogeneity in a single vein-type uranium ore deposit: Implications for nuclear forensics," *J. Environ. Radioact.*, vol. 150, pp. 75–85, Dec. 2015, doi: 10.1016/j.jenvrad.2015.06.016.

[26] G. Lu, A. J. Haes, and T. Z. Forbes, "Detection and identification of solids, surfaces, and solutions of uranium using vibrational spectroscopy," Nov. 01, 2018, *Elsevier B.V.* doi: 10.1016/j.ccr.2018.07.010.

[27] P. Duan, D.-Y. Lin, W.-T. Yang, X.-J. Huang, A.-H. Sun, and Q.-H. Pan, "Facile preparation of covalent organic frameworks@alginate composite beads for enhanced uranium(VI) adsorption", doi: 10.1007/s12598.

[28] Z. D. Li, H. Q. Zhang, X. H. Xiong, and F. Luo, "U(VI) adsorption onto covalent organic frameworks-TpPa-1," *J. Solid State Chem.*, vol. 277, pp. 484–492, Sep. 2019, doi: 10.1016/J.JSSC.2019.06.044.

[29] Y. Wu *et al.*, "Reversible Amine-to-Imine Chemistry at a Covalent Organic Framework for Sustainable Uranium Redox Separation," *ACS Sustain. Chem. Eng.*, vol. 12, no. 17, pp. 6659–6665, Apr. 2024, doi: 10.1021/acssuschemeng.4c00358.

[30] W. Rudzinski and W. Plazinski, "Kinetics of solute adsorption at solid/solution interfaces: A theoretical development of the empirical pseudo-first and pseudo-second order kinetic rate equations,

based on applying the statistical rate theory of interfacial transport," *Journal of Physical Chemistry B*, vol. 110, no. 33, pp. 16514–16525, Aug. 2006, doi: 10.1021/jp061779n.

[31] J. P. Vareda, "On validity, physical meaning, mechanism insights and regression of adsorption kinetic models," Apr. 15, 2023, *Elsevier B.V.* doi: 10.1016/j.molliq.2023.121416.

[32] Q. Li, L. Chai, Z. Yang, Q. Wang, and Y. Wang, "A Comparative Study of Ag(I) Adsorption on Raw and Modified Spent Grain: Kinetic and Thermodynamic Aspects," *Water Environment Research*, vol. 82, no. 11, pp. 2290–2296, Nov. 2010, doi: 10.2175/106143010x12681059116978.

[33] M. I. El-Khaiary, G. F. Malash, and Y. S. Ho, "On the use of linearized pseudo-second-order kinetic equations for modeling adsorption systems," *Desalination*, vol. 257, no. 1–3, pp. 93–101, Jul. 2010, doi: 10.1016/j.desal.2010.02.041.

[34] J. Wang and X. Guo, "Adsorption isotherm models: Classification, physical meaning, application and solving method," Nov. 01, 2020, *Elsevier Ltd*. doi: 10.1016/j.chemosphere.2020.127279.

[35] I. Langmuir, "The constitution and fundamental properties of solids and liquids," *J. Am. Chem. Soc. 38*, no. 2221–2295, 1916.

[36] X. Guo and J. Wang, "Comparison of linearization methods for modeling the Langmuir adsorption isotherm," *J. Mol. Liq.*, vol. 296, Dec. 2019, doi: 10.1016/j.molliq.2019.111850.

[37] Y.-S. Ho, "Isotherms for the Sorption of Lead onto Peat: Comparison of Linear and Non-Linear Methods," 2006.

[38] T. W. Weber, R. K. Chakravorti, and R. K. Chakravorti, "Pore and Solid Diffusion Models for Fixed-Bed Adsorbers," 1974. doi: https://doi.org/10.1002/aic.690200204.

[39] H. Heshmati, M. Torab-Mostaedi, H. Ghanadzadeh Gilani, and A. Heydari, "Kinetic, isotherm, and thermodynamic investigations of uranium(VI) adsorption on synthesized ion-exchange chelating resin and prediction with an artificial neural network," *Desalination Water Treat.*, vol. 55, no. 4, pp. 1076–1087, Jul. 2015, doi: 10.1080/19443994.2014.922495.

[40] H.M.F. Freundlich, "Over the adsorption in solution," *J. Phys. Chem. 57* , pp. 385–471, 1906.

[41] C. R. Girish, "Determination of thermodynamic parameters in adsorption studies: a review," Sep. 01, 2025, *Springer Science and Business Media Deutschland GmbH*. doi: 10.1007/s11696-025-04218-x.

[42] H. N. Tran, "Improper Estimation of Thermodynamic Parameters in Adsorption Studies with Distribution Coefficient K D(q e/ C e) or Freundlich Constant (K F): Considerations from the Derivation of Dimensionless Thermodynamic Equilibrium Constant and Suggestions," *Adsorption Science and Technology*, vol. 2022, 2022, doi: 10.1155/2022/5553212.

[43] M. A. Islam, M. K. Nazal, A. A. Akinpelu, M. Sajid, N. A. Alhussain, and M. Ilyas, "High-performance adsorptive removal of emerging contaminant paracetamol using a sustainable biobased mesoporous activated carbon prepared from palm leaves waste," *J. Anal. Appl. Pyrolysis*, vol. 180, Jun. 2024, doi: 10.1016/j.jaap.2024.106546.

[44] S. Paik, S. K. Satpati, and D. K. Singh, "Nucleation kinetics of reactive crystallization of ammonium di-uranate," *Indian Chemical Engineer*, vol. 65, no. 6, pp. 527–542, 2023, doi: 10.1080/00194506.2023.2223605.

[45] Y. Xie *et al.*, "Uranium extraction from seawater: material design, emerging technologies and marine engineering," Nov. 30, 2022, *Royal Society of Chemistry*. doi: 10.1039/d2cs00595f.

[46] J. Ma, T. Zhang, and F. Yu, "Progress and Prospect of covalent organic frameworks for uranium (VI) adsorption and conversion from aqueous sources," Jun. 01, 2026, *Elsevier B.V.* doi: 10.1016/j.ccr.2026.217641.